Measurement-based Analysis of Delay-Doppler Characteristics in an Indoor Environment

Brecht Hanssens, Emmeric Tanghe, Luc Martens,
Claude Oestges and Wout Joseph

***Abstract*—An analysis of delay-Doppler characteristics in the presence of moving people is presented for short-range communication in an indoor environment. Channel sounding measurements have been carried out at 3.6 GHz in a crowded university hall during several short and long breaks in-between courses. During three consecutive days, the measurements were repeated with different positions for the transmit and receive antennas. In this study, the behavior of the maximum Doppler shift and the Doppler spread were analyzed in the time-delay domain as a function of the occupation of the hall, the polarizations of the 2×2 MIMO antennas, and their positions in the hall. The measurements reveal a clear distinction between the Doppler spread of the short and long breaks in the campaign, indicating a distinctive power distribution of their Doppler spectra. In addition, there is a significant contrast between the Doppler characteristics of the co- and cross-polarizations. Measurements at several positions reveal the importance of characterizing multipaths, and show that the Doppler effect depends on the position of the antennas in the environment. In addition, this work also shows that the Doppler spectrum can be accurately modeled by a Cauchy distribution, allowing for the generation of parameters to describe Doppler characteristics.**

***Index Terms*—Channel Sounding & Modeling, Delay-Doppler, Multipath Propagation, Polarization, Indoor Environment**

I. Introduction

Indoor radio channels are commonly characterized by multipath propagation phenomena such as reflection, diffraction, and scattering. As such, the channel transfer function includes contributions of several attenuated and delayed versions of the original transmitted signal. Over time, movement of the transmitter, receiver and/or obstacles encountered in the radio channel, will give rise to phase changes of the propagation paths. Apart from small and large-scale fading, these phase shifts are the main cause of the time-variability in the channel transfer function. Movement in the radio channel will also broaden the frequency spectrum of the received signal, resulting in a frequency shift between the transmitted and received signal. These shifts are referred to as Doppler shifts, and the weighted standard deviation of their distribution is known as the Doppler spread. The Doppler spread provides insight into the distribution of power in the Doppler spectrum, and hence relates to the different Doppler frequency shifts (speeds or path elongations) which can be found in the radio channel. Higher Doppler spreads can thus be seen as more randomness in the movement of scatterers between transmitter and receiver. Next to that, the maximum Doppler shift is considered to be the highest Doppler frequency shift resulting from realistic scattering phenomena in the radio channel.

Doppler spreading is inherently proportional to the carrier (or subcarrier) frequency of such a communication system, as the time-selective fading is also frequency-dependent. Narrowband systems relying on frequency multiplexing will suffer less from this effect, as the fading can be assumed uniform over all subcarriers. However, in e.g., Orthogonal Frequency Division Multiplexing (OFDM) or Ultra-Wideband (UWB) communication systems, the different subcarriers on which the information is modulated are more widely spaced in the frequency domain. As illustrated in [1], the minimum required subcarrier spacing of a communication system is chosen in function of the guard time, where this spacing should at least equal the maximum realistic Doppler shift encountered in the radio channel. This will in turn have an impact on the useful spectrum occupancy rate of such a system, as broader spectra result in a larger spacing of the different subcarriers. It should also be noted that in current channel models, e.g. COST 2100 [2], the impact of the Doppler effect of user motion on the channel capacity is neglected, as this model only takes receiver motion into account. Next to that, an accurate estimation of Doppler shifts is of high importance in system design to improve detection, as the receiver needs to tune to a certain carrier frequency subjective to Doppler shifts.

The objective of this work is the analysis of delay-Doppler characteristics of a dynamic indoor environment at 3.6 GHz in a crowded university hall (see Fig. 1), and this during several short and long breaks in-between classes with varying occupational densities (i.e., amount of people). In addition, we will also take a look at the impact of different polarizations on these Doppler characteristics, as well as assess the influence of the various measurement positions in our indoor scenario.

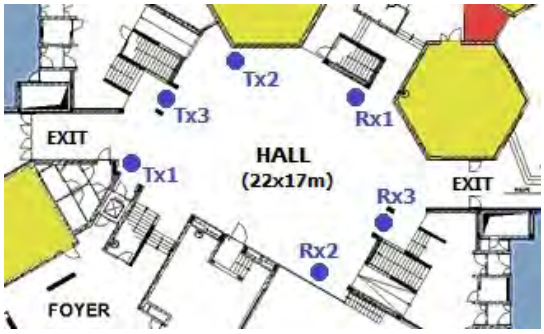

Figure 1: Measurement environment with the positions of the transmit and receive antennas marked in dots. Their indices correspond with the days of measuring; Tx_1-Rx_1 is 15.26m, Tx_2-Rx_2 is 19.75m and Tx_3-Rx_3 is 18.16m

Over the course of three days, the indoor radio channel was probed with a channel sounder to capture Doppler shifts caused by moving scatterers in the time-delay domain. On each day, both the transmit and receive antennas occupied different stationary locations across the hall, in order to assign the time-variant behavior of the channel to the movement of people. The novelty is that we will investigate whether different measurement positions, as well as varying distances between both antennas, have an impact on the characteristics of the delay-Doppler spectrum. A second and important novelty is the full polarimetric analysis of these Doppler characteristics. Although temporal variations of the indoor radio channel were previously described in [3]–[5], the impact of polarization on these variations was still omitted in these works.

B. Hanssens, E. Tanghe, L. Martens and W. Joseph are with iMinds-WiCa, Ghent University, Belgium, e-mail: Brecht.Hanssens@INTEC.UGent.be
C. Oestges is with ICTEAM, Catholic University of Louvain, Belgium

II. Measurements

A. Measurement environment

The indoor measurements were carried out during school hours in a crowded university hall of the Université Catholique de Louvain (UCL) in Louvain-la-Neuve, Belgium. Fig. 1 depicts the measurement environment, as well as the fixed positions of the transmit and receive antennas in our measurement campaign. The university hall is approximately $22\times17\times3$ meters, and occupied at most by 200 people (depending on the courses that were given at the time of measuring). There are two main exits to the hall, which are both indicated on the left and right of the figure. Several smaller hallways lead to various sizes of auditoriums, indicated in blue and yellow.

(a) Short break **(b)** Long break

Figure 2: Occupation of the measurement environment.

During each of the three measurement days, four blocks of two hour-long courses were given in the auditoriums adjacent to the hall, all separated by a mandatory 'long' break. Some time before and after these courses, we can thus expect plenty of movement in the hall. During each course, a 'short' break of about 10 minutes was given optionally by the lecturers. However, these breaks are non mandatory, and occur approximately half-way during a class. Furthermore, because these breaks also vary in duration, we can expect fewer students per measurement cycle in the hall during these type of breaks.

B. Channel sounding procedure

Indoor measurements were carried out with an Elektrobit channel sounder at a carrier frequency of 3.6 GHz with a bandwidth of 200 MHz. At the transmitter (Tx) side, a horn antenna was used, which had both horizontal and vertical polarizations. Two custom-made 45° slanted patch antennas were used at the receiver (Rx) side of the system. The channel sounder employs a long pseudo-noise sequence to estimate the channel impulse response for the full polarimetric channel.

III. Evaluation

At each of the 315 time-delay samples per polarization (one measurement cycle), the channel sounder measures the S_{21}-scattering parameter between all possible configurations of transmitting and receiving antennas. We can excite the H- and V-polarizations with the horn antenna at the Tx-side, and recalculate the H- and V-contributions from the complex S_{21}-parameters measured at the Rx-side. This 2×2 Multiple-Input Multiple-Output (MIMO) scenario lets us thus estimate the impulse response of the full polarimetric indoor radio channel, that is, between the VV-, HH-, HV- and VH-polarizations (e.g., 'HV' corresponds to the transmitted H-polarization, and the received (45°-projected) V-polarization).

In order to calculate a delay-Doppler spectrum from which we can estimate the maximum Doppler shift and the Doppler spread, a certain number of measurement cycles has to be combined. Every MIMO-matrix (four polarizations with each 315 samples) will capture 8 ms of data, corresponding with a maximum measurable Doppler shift of 125 Hz. Combining too low amount of cycles will result in a poor spectral resolution, however, when combining too much cycles, the channel can no longer be assumed stationary. In [6], the correlation distance metric was introduced to characterize the stationarity between two time instances, which can be interpreted as the measure of the overlap in signal space between two correlation matrices, and thus measures their orthogonality. This metric can be reformulated as the collinearity, and applied to power spectral densities which are directly related to the correlation function by means of the Fourier transform. This results in a strictly bounded metric that compares the channel impulse response at different time instances. To decide how many cycles to combine, we analyzed the stationarity time in the channel [7], which is the time range where the collinearity between two measurements exceeds a given threshold. Doing so, we have chosen to combine a total of 4 s of data from which we can calculate a delay-Doppler spectrum. This is the equivalent of 501 consecutive cycles, allowing us to obtain a Doppler spectral resolution of 0.5 Hz. The spectrum combining both time-delay (ranging from 0 to 630 ns) and Doppler frequency shifts (ranging from -125 to 125 Hz) was then calculated by making use of the discrete Fourier transform.

The maximum Doppler frequency shift f_D and Doppler spread f_{RMS} per delay bin is then based on the range of Doppler shifts over which the power spectrum is non zero. However, such a spectrum will never be truly zero due to measurement uncertainties, noise generated by the channel sounder, etc. In our analysis, the maximum Doppler shift is the frequency shift for when the power first drops below a certain threshold, which was chosen as the average noise Doppler power, plus an additional 6 dB in order to stay clear from the noisy part of the spectrum.

IV. Results

A. Influence of occupational density on Doppler parameters

As previously mentioned and as shown in Fig. 2, there are two types of breaks in a typical day: short (low occupation) and long (high occupation). During both types of breaks, the hall is comprised of a combination of people moving, and those standing still making conversation. Most of the time, both behaviors tend to appear in group (i.e., clusters of people).

Fig. 3 shows the median value for the maximum delay-Doppler shift estimate of the VV-polarization for the Tx_1-Rx_1 link, for both the long and short breaks in-between courses.

Maximum Doppler shifts of 36 Hz and 40 Hz were measured at the first arriving multipath component for the long and short breaks, respectively. This indicates that people move faster during the short breaks, rather than during the long ones. Looking at the second arriving multipath component, we can

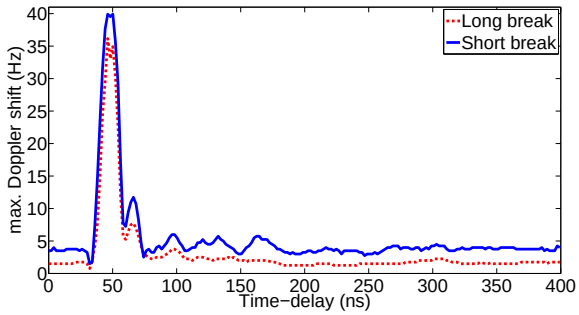

Figure 3: Maximum delay-Doppler shift estimate for both the long and short breaks in-between courses. Configuration: Tx_1-Rx_1 link, and VV-polarization.

still observe maximum Doppler shifts of 8 Hz and 12 Hz for the long and short breaks respectively. Later arriving multipath components correspond to longer paths from transmitter to receiver, e.g., reflections on walls. It should be noted that a lot of people were standing still towards the side of the hall, in contrast to the center where the majority of the people were moving from one side to another. This corresponds well with our observation of increasingly lower values for the maximum Doppler shift at later arriving multipath components.

B. Influence of polarization on Doppler parameters

Fig. 4 shows the maximum delay-Doppler shift estimate for the full polarimetric radio channel, averaged over all the long breaks in the Tx_1-Rx_1 link.

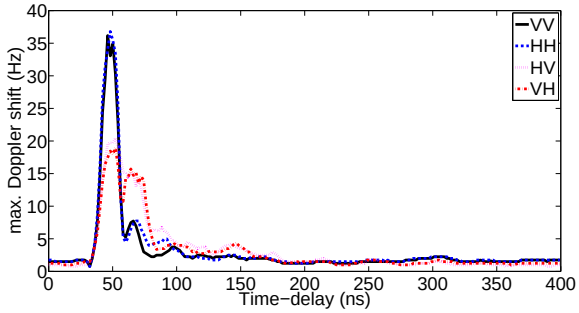

Figure 4: Median of all estimated maximum Doppler shifts for the full polarimetric radio channel. Configuration: Tx_1-Rx_1 link, long break.

When studying the first arriving multipath component at 50 ns, we measured maximum Doppler shift for both VV- and HH-polarizations of approximately 36 Hz. The Doppler values for these two co-polarizations (VV and HH) differ quite strongly with those of both cross-polarizations (HV and VH), which were only about 20 Hz (see also Table I). We can thus state that there is a significant difference between the Doppler characteristics of co- and cross-polarizations in this specific link. However, looking at the second arriving multipath component at 70 ns, the cross-polarized waves still result in maximum Doppler shifts that are comparable with those of the first arriving components (15 Hz), whereas the co-polarizations only reaches values of 8 Hz.

C. Influence of measurement positions on Doppler parameters

Fig. 5 presents the median of all maximum Doppler shifts for the VV-polarization during the short breaks over the three positions. For comparison, each Tx-Rx link is shifted in the delay domain so their peak-values align at 50 ns; the delay of the first arriving multipath component of the Tx_1-Rx_1 link.

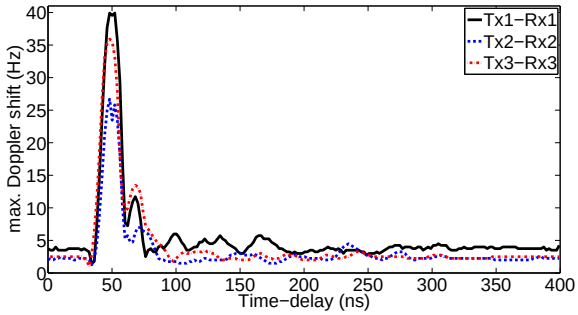

Figure 5: Estimated maximum Doppler shifts for the three measurement positions. Each graph is shifted in the delay domain for comparison so their peak values align at 50 ns. Configuration: VV-polarization, short break.

Varying results over the three positions can be explained by different multipath phenomena such as reflection, diffraction, and scattering. There is a clear effect in the Tx_1-Rx_1 and Tx_3-Rx_3 link, where the maximum Doppler shift is still reasonably high for the second arriving component with corresponding values of 11.7 Hz and 13.5 Hz. The lower spread in the Tx_2-Rx_2 link can be explained by the fact that both transmitter and receiver are located relatively far from the exits of the hall, and thus fewer movement happens near both antennas compared to the Tx_1-Rx_1 and Tx_3-Rx_3 link.

D. Summary of the measurement results

Table I lists an analysis of the maximum Doppler shifts and -spreads for the polarimetric radio channel. All polarizations are compared against each other throughout the short and long breaks in our campaign. Next to that, the influence of different measurement positions is examined. The values in the table represent the maximum value in the time-delay domain of the median estimated maximum Doppler shift response per configuration (e.g., VV, Tx_1-Rx_1, median{short breaks}).

		Tx_1-Rx_1 (15.3m)		**Tx_2-Rx_2** (19.8m)		**Tx_3-Rx_3** (18.2m)	
		short	long	short	long	short	long
VV	f_D	39.92	36.18	26.70	31.94	35.93	39.17
	f_{RMS}	10.35	23.73	10.12	12.23	8.47	13.35
HH	f_D	40.79	36.80	26.32	33.31	36.43	39.8
	f_{RMS}	10.79	22.77	10.09	12.56	8.46	13.17
HV	f_D	27.94	20.46	19.84	28.82	32.68	37.92
	f_{RMS}	8.53	13.52	8.41	11.74	8.23	13.94
VH	f_D	28.19	18.96	18.71	27.94	29.94	37.67
	f_{RMS}	8.56	12.31	8.45	12.13	7.50	14.21

Table I: Comparison of maximum Doppler shifts and -spreads (Hz) for the full polarimetric indoor radio channel, throughout the various short and long breaks in our campaign, as well as over the different measurement positions.

From this table, we can conclude that there is a significant difference between short and long breaks in-between courses. Looking at the short breaks for the Tx_1-Rx_1 link, their maximum Doppler shifts will always result in significantly higher values than the long breaks, thus representing faster movement in the radio channel. For the Tx_2-Rx_2 and Tx_3-Rx_3 link,

this is not the case anymore. More noticeable, the maximum Doppler shift of the short breaks is compellingly lower in these scenarios. Looking at the behavior of the Doppler spread, we can state that the Doppler power during the short breaks is strongly concentrated towards the center of the spectrum. This can be explained by the observation that during the long breaks, there are a lot of people present in the channel due to the fact that they all have to switch courses, and thus have to cross the hall. More people also means that there are a lot of various walking speeds and orientations towards the antennas, and thus a higher Doppler spread.

When comparing polarizations, we can easily observe that the co-polarizations (VV and HH) tend to result in broader Doppler characteristics than the cross-polarizations (HV and VH). The Doppler characteristics are also very position-dependent. For example, the maximum Doppler shifts and -spreads are consistently lower for the Tx_2-Rx_2 link than for the Tx_1-Rx_1 and Tx_3-Rx_3 link. This can be explained by the fact that the movement of people in the environment happens mostly in the vicinity of the antennas for the latter two links, as they are closer to the exits of the university hall.

E. Modeling the delay-Doppler spectrum

In this section, we compare three possible maximum likelihood estimates to model the delay-Doppler spectrum with respect to Doppler frequency shift. The models in this paper are based on a Cauchy-, a Laplace- and a Gaussian (normal) distribution. All these functions have four tunable parameters, which makes them easy to compare against each other.

- Cauchy: $D(f_d) = \frac{a}{\pi\, b\left(1+\frac{f_d-c}{b}\right)^2} + d$
- Laplace: $D(f_d) = \frac{a}{2b}\exp\left(-\frac{|f_d-c|}{b}\right) + d$
- Gaussian: $D(f_d) = \frac{a}{\sqrt{2\pi\, b^2}}\exp\left(\frac{-(f_d-c)^2}{2\,b^2}\right) + d$

with a, b, c and d representing the parameters of each model, f_d the Doppler frequency shift, and $D(f_d)$ the Doppler power.

In order to find the best fitting distribution for the Doppler spectrum, we have searched for the lowest root-mean-square error between the measured data and these three functions. In order to avoid computational complexity, only the three most dominant multipath components were used to model the Doppler spectrum, extracted through visual inspection in the time-delay domain. We found that the Cauchy distribution is the best possible fit in most cases for all Tx-Rx links, acting as the best possible fit in over 70% of the cases. Looking at the difference between short and long breaks in our campaign, we can carefully argue that the Cauchy distribution becomes steadily less important to model the latter type of breaks, albeit being still much better than the Laplace distribution.

Table II subsequently shows an analysis of the parameters a, b, c and d of the Cauchy distribution. Looking at the results of the shape-dependent parameter b of this model, we can see that both the median and standard deviation are consequently lower for the short- than for the longer breaks. This agrees perfectly well with our observation of lower Doppler spreads for these respective types of breaks, indicating that the Doppler power is strongly concentrated towards the center of the spectrum.

		a		**b**		**c**		**d**	
		median	stdvar	median	stdvar	median	stdvar	median	stdvar
VV	short	44.08	20.04	0.38	0.18	-0.01	0.05	-57.99	7.22
	long	49.43	52.45	0.43	0.50	-0.36	0.21	-48.27	5.81
HH	short	46.25	25.26	0.38	0.18	-0.01	0.06	-56.47	6.42
	long	40.67	65.77	0.39	0.62	-0.39	0.21	-47.67	5.98
HV	short	54.47	85.86	0.45	0.80	-0.01	0.07	-45.19	5.25
	long	54.54	111.31	0.47	1.21	-0.44	0.22	-38.42	5.69
VH	short	58.74	50.51	0.46	0.43	-0.01	0.06	-45.64	5.59
	long	52.62	116.44	0.47	1.17	-0.39	0.26	-37.66	6.00

Table II: Parameter analysis of the Cauchy distribution model for the full polarimetric radio channel, throughout short and long breaks. Indicated are the median and standard deviation of each parameter for the Tx_1-Rx_1 link.

V. Conclusions

This work presents an analysis of delay-Doppler characteristics at 3.6 GHz in a crowded university hall. Both the maximum Doppler shift and Doppler spread were evaluated in the time-delay domain as a function of the occupational density of the hall, as well as the polarizations and positions of both transmit and receive antennas. Measurements at three different positions reveal the importance of multipath phenomena and occupational density on the Doppler characteristics, and demonstrate the difference between those of the co- and cross-polarizations. We also propose the Cauchy distribution as the best fit to model the Doppler frequency spectrum. An analysis of the shape dependency of this model provides comparable results to those of the Doppler spread.

Future work includes an enhancement of the COST 2100 channel model [2] with Doppler characteristics for user motion, and an evaluation of the effect of antenna de-embedding.

Acknowledgment

Brecht Hanssens is funded by the Agency for Innovation by Science and Technology in Flanders (IWT). Emmeric Tanghe is funded by the Research Foundation Flanders (FWO). This research was supported by the project IUAP BESTCOM, "BElgian network on STochastic modelling, analysis, design and optimization of COMmunication systems". This work was partly funded by the FWO project 3G027714.

References

[1] I. R. Capoglu, Y. Li, and A. Swami. Effect of Doppler spread in OFDM-based UWB systems. *IEEE Transactions on Wireless Communications*, 4(5):2559–2567, 2005.

[2] R. Verdone and A. Zanella. *Pervasive Mobile and Ambient Wireless Communications: COST Action 2100*. Signals and Communication Technology. Springer, 2012.

[3] A Domazetovic, L. J. Greenstein, N. B. Mandayam, and I Seskar. Estimating the Doppler Spectrum of a Short-Range Fixed Wireless Channel. *IEEE Communications Letters*, 7(5):227–229, 2003.

[4] P. Pagani and P. Pajusco. Characterization and Modeling of Temporal Variations on an Ultrawideband Radio Link. *IEEE Transactions on Antennas and Propagation*, 54(11):3198–3206, 2006.

[5] H. P. Bui, H. Nishimoto, Y. Ogawa, T. Nishimura, and T. Ohgane. Channel Characteristics and Performance of MIMO E-SDM Systems in an Indoor Time-varying Fading Environment. *EURASIP Journal on Wireless Communications and Networking*, 44:1–13, 2010.

[6] M. Herdin, N. Czink, H. Ozcelik, and E. Bonek. Correlation Matrix Distance, a Meaningful Measure for Evaluation of Non-Stationary MIMO Channels. In *IEEE Vehicular Technology Conference*, pages 136–140, 2005.

[7] L. Bernadó. *Non-Stationarity in Vehicular Wireless Channels*. PhD thesis, Technische Universität Wien, Vienna, Austria, 2012.